

- Benchmark case -

**Single dowel-type connection tensile test with slotted-in steel plate**

**1 Objectives**

This benchmark aims to offer reference values for the FE modelling of tensile tests on steel-timber dowel-type connections with a single fastener regarding

- the load-displacement curve and
- the related connection stiffness.

This benchmark's data sheets and analytical reference results are based on the work of KUHLMANN & GAUB [4].

**2 Description of the Beam on Foundation (BoF)-model**

**2.1 Overview**

In this benchmark, the steel-timber dowel-type connection of the test no. *G-SD16 11 0 2 2* (see Fig. 1) is modelled in RFEM (Dlubal) using a Beam on Foundation (BoF)-model. The model shown in Fig. 1 (right) and Fig. 2 based on the approach presented by HOCHREINER ET AL. [2] and expanded by SCHWEIGLER [5].

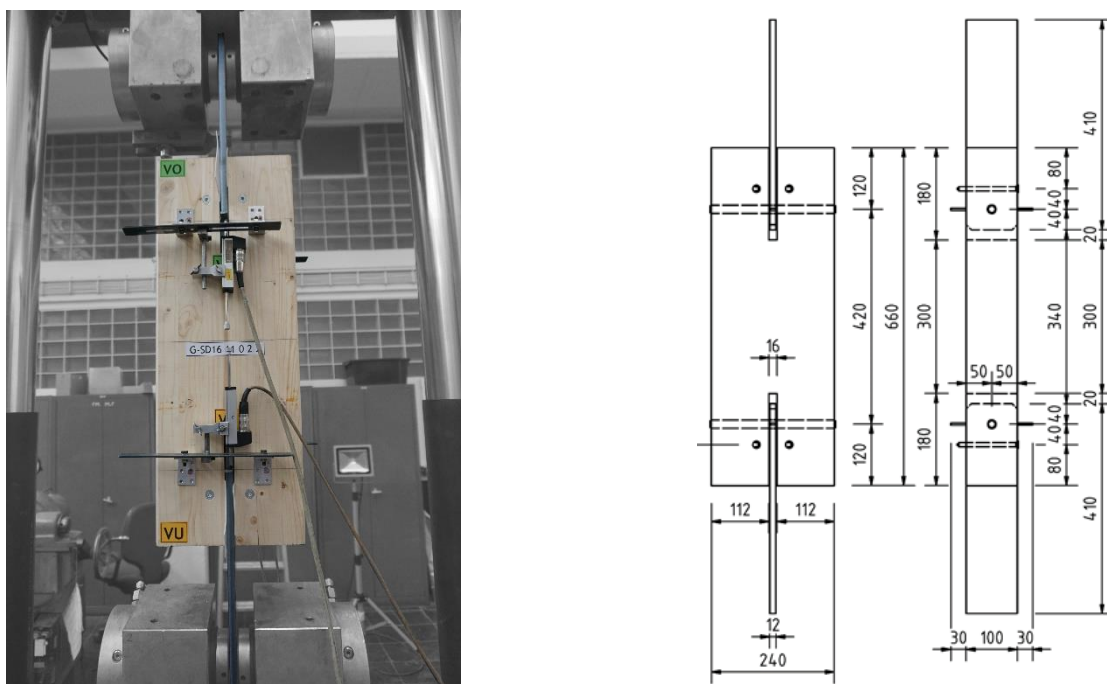


**Fig. 1:** Test setup of the single dowel-type connection tensile test with slotted-in steel plate no. *G-SD16 11 0 2 2* (left) and geometry of the test specimen (right) [4]

Fig. 2 gives an overview of the main components and node properties of the BoF-model and defines the coordinate system. The main components of the model are described in more detail below.

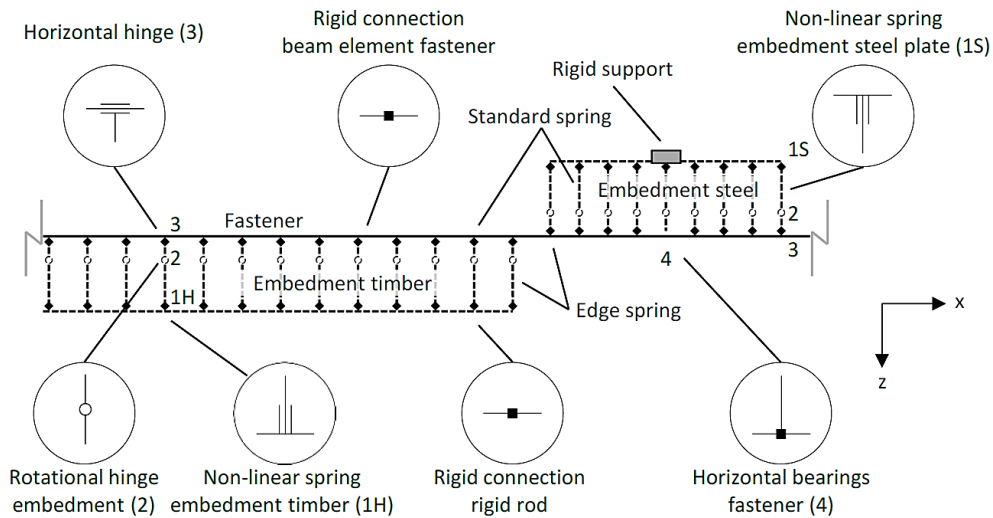


**Fig. 2:** Overview of the main components of the BoF-model and definition of the coordinate system [3]

## 2.2 Non-linear spring “embedment timber“ (1H)

The embedment of the fastener in the timber has a significant influence on the load-deformation behaviour of the connection. In the model, the embedment in the timber is modelled by non-linear springs. For this purpose, rigid rods are evenly spaced and supported at position 1H (see Fig. 2) in such a way that only deformation in the global z-direction is permitted. The other two displacements and all rotations are fixed. The deformation in global z-direction is characterised by a non-linear load-deformation diagram and describes the embedment behaviour of the fastener in the timber. The embedment properties can be represented approximately by the following parameterised curve according to equation (1) and are specified in the model by nine individual points. For more detailed explanations of equation (1) see also SCHWEIGLER [5].

$$f_h(u) = \frac{(k_{ser} - k_f) \cdot u}{\left[1 + \left[\frac{(k_{ser} - k_f) \cdot u}{f_{h,int}}\right]^\alpha\right]^{\frac{1}{\alpha}}} + k_f \cdot u \quad (1)$$

with:	$f_h$	Embedment stress [N/mm <sup>2</sup> ]
	$u$	Displacement in the embedment zone [mm]
	$k_{ser}$	Initial stiffness [N/mm/mm <sup>2</sup> ]
	$k_f$	End gradient of the slip curve [N/mm/mm <sup>2</sup> ]
	$f_{h,int}$	Embedment stress at intersection of the tangent from $k_f$ with the vertical axis [N/mm <sup>2</sup> ]
	$\alpha$	Transition parameter [-]



The implemented spring properties are a function of the load-bearing area of the respective spring. The load-bearing area of the spring results from the contact length between the fastener and the (timber-) element (distance of the springs in global x-direction) and the diameter of the fastener. Since the springs at the edges of the timber element only have half the contact length compared to the springs in the middle, the spring properties have to be adjusted accordingly. A distinction is therefore made between edge and standard springs. [4]

### 2.3 Non-linear spring “Embedment steel plate” (1S)

The modelling of the flexibility of the contact between fastener and slotted-in steel plate is carried out according to the same principle as the modelling of the contact between fastener and timber through the arrangement of non-linear springs, whereby a distinction is made between standard and edge springs as well. The deformations of the slotted-in steel plate in the embedment area are to be considered very low compared to those of the timber in the embedment area. However, since the fastener is highly stressed due to the rigid support in the area of the slotted-in steel plate and the multiaxial state of stress (bending, shear, contact pressure), visible plastic indentations of the slotted-in steel plate into the fastener already occur at relatively small bending angles. In order to be able to take this yielding into account in the numerical model, the required spring properties were determined by 3D FE modelling in ANSYS (Workbench 18.0). A detailed description of these FE investigations is given in [4].

### 2.4 Modelling of the fastener

The fastener is modelled as a continuous beam element with a circular cross-section. The "Isotropic nonlinear elastic 1D" model in RFEM is used as the material model. The experimentally determined material properties are taken into account by 12 individual points in a non-linear stress-strain curve. The stress-strain curve of the fasteners was determined for the diameters 8 mm, 12 mm, 16 mm and 20 mm by tensile tests on a randomly taken sample. The results of the tensile tests are listed in [1], [3] and [4].

### 2.5 Rotational hinge embedment (2) and horizontal hinge (3)

A moment hinge (2) is placed below the beam element (fastener) at a distance of 1 mm, which enables rotation of the fastener axis. This allows the force transmission between the beam element and the embedment to always be perpendicular to the fastener axis. To avoid undesirable force components when the fastener is twisted, the distance between the hinge and the fastener axis should be sufficiently small. The beam element is coupled to the embedment springs by means of a hinge (3) that can be moved in the longitudinal direction of the fastener. The other two displacements and the rotations are rigidly connected. To prevent the entire system from becoming kinematic, the beam element is supported centrally in a non-displaceable manner (4). The horizontal hinge also allows the modelling of friction between the fastener and the embedment area. However, it was shown that the influence of friction is negligible for non-profiled fasteners, so that a frictionless support is always assumed for this benchmark case. [4]





## 2.6 Rigid rod

The individual non-linear springs in the embedment areas are connected by rigid rods and thus connected in parallel. The rigid rods are connected to the support (or, if necessary, to other fasteners) by further rigid rods. These rigid rods receive an elastic flexibility in the longitudinal direction, which is calculated according to equation (2).

$$K_{coupling} = \frac{(E \cdot A)}{a_{3,t}} \quad (2)$$

with:  $E$  Mean E-modulus of the timber member [N/mm<sup>2</sup>]  
 $A$  Cross-sectional area side member [mm<sup>2</sup>]  
 $a_{3,t}$  End grain distance [mm]

In this way, influences from deformations of the timber matrix can be directly taken into account in the model. A comparison of the connection stiffnesses from embedment tests as compression tests and from component tests as tension tests resulted in a deviation of the stiffnesses, so that a reduction of the side member stiffness according to equation (2) by 1/3 is carried out. However, the effect of this flexibility on the load-deformation curve of the connection is to be regarded as small. [4]

## 3 Geometry definition and discretization

Tab. 1 summarises the relevant geometry parameters as well as the chosen discretisation for the BoF-model.

The discretisation is carried out depending on the position of the non-linear springs by individual finite elements in between. For this reason, the springs should be evenly distributed. In addition, the distance between the individual springs should be sufficiently small. It should be noted that the side member thickness should be a multiple of the selected spring spacing in order to avoid convergence problems. Comparative calculations showed that spring distances between 1 and 3 mm are advantageous. Larger spring distances lead to inaccuracies in the calculation results, while smaller distances can no longer be modelled exactly in RFEM.



**Tab. 1:** Input values to define the geometry and the discretization of the BoF-model

Input parameter	Short name	Value	Unit
Discretization side member 1	$x_1$	2	mm
Discretization side member 2	$x_2$	2	mm
Discretization steel plate	$x_3$	1.5	mm
Side member thickness 1	$t_1$	112	mm
Side member thickness 2	$t_2$	112	mm
Slot width	$b_{\text{slot}}$	16	mm
Width steel plate	$b_{\text{plate}}$	12	mm
Fastener diameter	$d$	16	mm
End grain distance	$a_{3t}$	120	mm
Edge distance	$a_4$	50	mm
Number of fasteners in z-direction	$n_z$	1	-
Number of fasteners in y-direction	$n_y$	1	-

## 4 Material properties

### 4.1 Embedment in timber

The input values given in Tab. 2 to define the embedment behaviour in timber have been determined as mean values in embedment tests.

**Tab. 2:** Experimentally determined mean values of important parameters describing the embedment in timber

Input parameter	Value	Unit
$k_{\text{ser}}$	49.0	N/mm/mm <sup>2</sup>
$k_f$	-0.5	N/mm/mm <sup>2</sup>
$f_{h,\text{int}}$	28.0	N/mm <sup>2</sup>
$u_0$	0.1	mm
$\alpha$	3.0	-

Using these values and equation (1), the experimentally determined embedment curve can be parameterised and described by 9 individual points, whereby the embedment stress is converted to a force using the embedment area of the fastener (correspond to the fastener diameter). Fig. 3 shows the values of the 9 points for the definition of the multilinear embedment behaviour in timber for standard and edge springs and the corresponding load-displacement diagram. The load-displacement curve is symmetrical to the origin. Furthermore, it should be noted that, as explained in chapter 2.2, the edge springs only have half the load-bearing area compared to the standard springs, so the force is also halved for the same displacement.

Displacement [m]	Load [kN]	
	Standard	Edge
0.00000	0.0000	0.0000
0.00015	0.0783	0.0391
0.00030	0.3091	0.1545
0.00050	0.5664	0.2832
0.00070	0.7219	0.3609
0.00100	0.8178	0.4089
0.00150	0.8547	0.4274
0.00230	0.8558	0.4279
0.00360	0.8350	0.4175

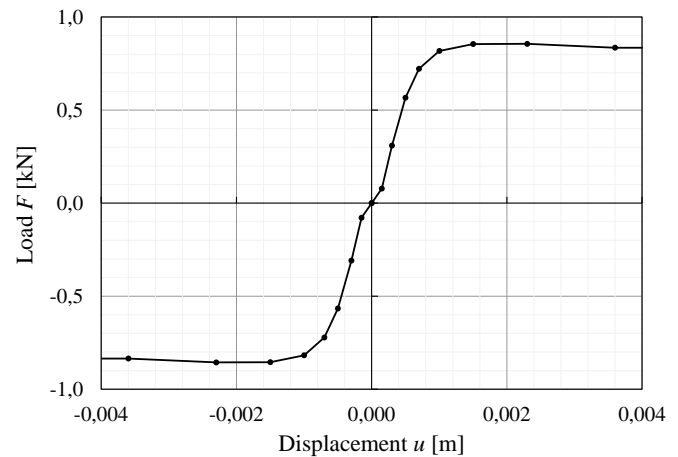


**Fig. 3:** Definition of the multilinear embedment behaviour in timber for standard and edge springs (left) and the corresponding load-displacement diagram (right)

## 4.2 Embedment in steel

In contrast to the embedment curve for timber, the embedment curve for steel is not symmetrical to the origin. The reason for this is the consideration of the dowel-hole clearance, which arises due to the always existing oversize of the hole in the slotted-in steel plate of 1 mm. The dowel-hole clearance is modelled by a forceless deformation of 1 mm in the transition from compression to tension. Thus, no tensile force can be transmitted between the fastener and the slotted-in steel plate in the contact area. The consideration of the dowel-hole clearance can also be seen in Fig. 4. The input values for the negative range of the embedment curve in steel are summarized in Tab. 3.

Displacement [m]	Load [kN]	
	Standard	Edge
0.00000	0.0000	0.0000
0.00100	0.1000	0.0500
0.00105	4.1310	2.0655
0.00109	7.6006	3.8003
0.00114	10.3560	5.1780
0.00123	13.8625	6.9313
0.00132	15.4575	7.7288
0.00141	16.3825	8.1913
0.00150	17.0200	8.5100
0.00163	17.7225	8.8613
0.00177	18.3788	9.1894
0.00190	18.6100	9.3050

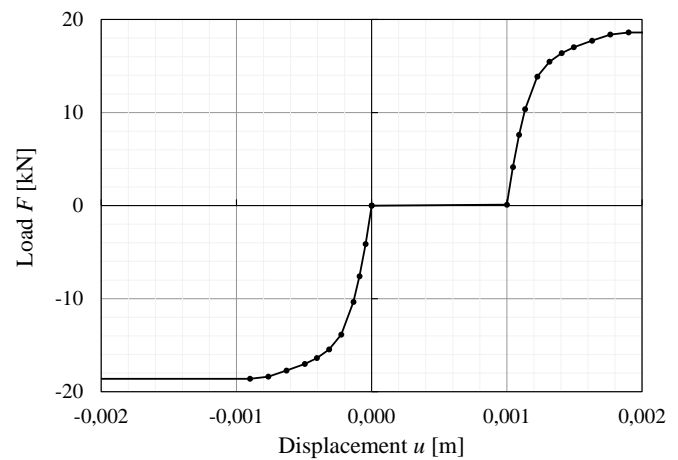


**Fig. 4:** Definition of the multilinear embedment behaviour in steel for standard and edge springs (positive range of the curve) (left) and the corresponding load-displacement diagram (right)



**Tab. 3:** Definition of the multilinear embedment behaviour in steel for standard and edge springs (negative range of the curve)

Displacement [m]	Load [kN]	
	Standard	Edge
0.00000	0.0000	0.0000
-0.00004	-4.1310	-2.0655
-0.00009	-7.6006	-3.8003
-0.00014	-10.3560	-5.1780
-0.00023	-13.8625	-6.9313
-0.00032	-15.4575	-7.7288
-0.00041	-16.3825	-8.1913
-0.00050	-17.0200	-8.5100
-0.00063	-17.7225	-8.8613
-0.00077	-18.3788	-9.1894
-0.00090	-18.6100	-9.3050





### 4.3 Material model steel

As mentioned in chapter 2.4, the experimentally determined material properties of the fastener are taken into account by 12 individual points in a non-linear stress-strain curve. The corresponding values as well as the stress-strain curve are given in Fig. 5. The stress-strain curve is symmetrical to the origin. It is important to note that the value for the stress  $\sigma_x$  of the second point in the curve must be compatible with the Young's modulus for steel. In this case,  $\sigma_x = 21.0 \text{ kN/cm}^2$  was chosen.

Strain $\varepsilon_x$ [-]	Stress $\sigma_x$ [kN/cm <sup>2</sup> ]
0.00000	0.0000
0.00100	21.0000
0.00357	70.9660
0.00395	75.4600
0.00518	80.3180
0.00755	82.7820
0.01166	84.0840
0.01582	84.2240
0.02213	84.9940
0.03074	85.4692
0.04779	86.2741
0.28000	100.8000

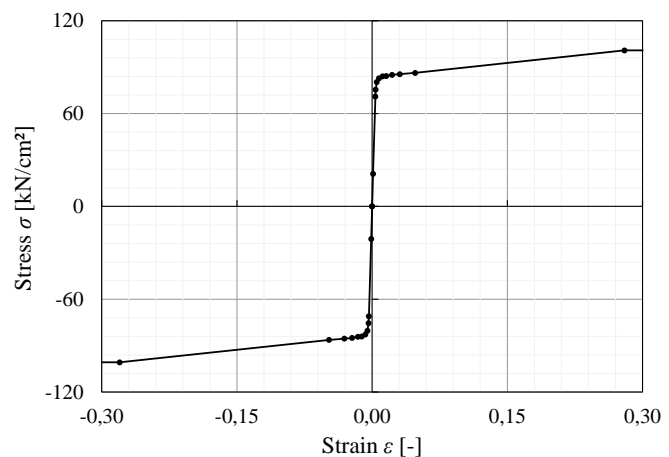


**Fig. 5:** Definition of the isotropic non-linear elastic material model for steel (left) and the corresponding stress-strain curve (right)

## 5 Loading and boundary conditions

The model is loaded by applying a displacement in global z-direction of  $z_u = -8 \text{ mm}$  at the middle node of the slotted-in steel plate.

The rigid rods connecting the embedment springs are supported non-displaceable (rigid support, see Fig. 2) at the slotted-in steel plate as well as in the area of the timber side members.

## 6 Calculation parameters

The following calculation parameters should be adjusted:

- Method of analysis: *Large deformation analysis*
- Method for solving system of nonlinear algebraic equations: *Newton-Raphson*
- Select the option “*save the results of all load increments*”
- Maximum number of iterations: *100*
- Number of load increments for load cases: *100*

For all other calculation parameters, the default settings can be used.

## 7 Experimental and numerical results

Fig. 6 compares the experimentally determined load-displacement curve and the corresponding stiffness with the numerically determined curves using the BoF-Modell in RFEM. The green curve (“Mean”) results from the input values according to Tab. 2, which were determined as mean values in the embedment tests. It can be seen that averaged input values already reproduce the connection behaviour well. Especially the initial stiffness can be reflected precisely by the model based on average values. A slight adjustment of individual embedment parameters, which can be justified by possible scattering of material properties and deviations of the (drill hole) geometry, leads to an even better agreement between experimentally and numerically determined load-displacement behaviour, in which the description of the plastic plateau in particular is optimised (see „RFEM“).

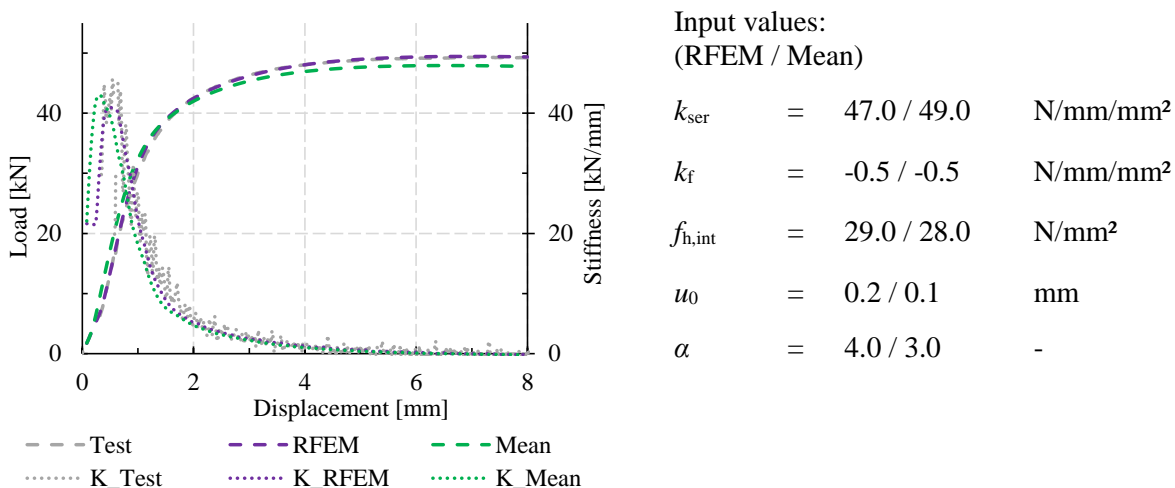


**Fig. 6:** Experimental (“Test”) and numerical (“RFEM” + “Mean”) load-displacement curves and related connection stiffness (Test no. *G-SD16 11 0 2 2*) [4]



## 8 References

- [1] KUHLMANN, U. & BUCHHOLZ, L. (2022): *Innovative Holzknotten durch Modellierung der Steifigkeit für leistungsfähige Holztragwerke aus Laub- und Nadelholz*. Forschungsvorhaben im Rahmen der Holzbau-Offensive des Ministeriums für Ländlichen Raum und Verbraucherschutz Baden-Württemberg, Institut für Konstruktion und Entwurf, Universität Stuttgart, laufend seit 2021.
- [2] HOCHREINER, G. ET AL. (2013): *Stiftförmige Verbindungsmittel im EC5 und baustatische Modellbildung mittels kommerzieller Statiksoftware*. In: Bauingenieur, 88, pp. 275 – 289.
- [3] KUHLMANN, U. & GAUB, J. (2019): *Stiffness of Steel-Timber Dowel Connections – Experimental and Numerical Research*. INTER, 54-7-9, Web-conference, Institute of Structural Design, University of Stuttgart.
- [4] KUHLMANN, U. & GAUB, J. (2021): *Wirtschaftliche Dimensionierung von Holztragwerken durch leistungsfähige Stahl-Holz-Stabdübelverbindungen*. IGF research project No. 20625 N (AiF/iVTH), Institute of Structural Design, University of Stuttgart.
- [5] SCHWEIGLER, M. (2018): *Nonlinear modelling of reinforced dowel joints in timber structures – a combined experimental-numerical study*. Dissertation, Vienna University of Technology.

